Surfaces, Interfaces, and Applications

Highly sensitive optical detection of Escherichia coli using Terbium based metal-organic framework

Arushi Gupta, Mayank Garg, Suman Singh, Akash Deep, and Amit L. Sharma

ACS Appl. Mater. Interfaces, **Just Accepted Manuscript** • DOI: 10.1021/acsami.0c14312 • Publication Date (Web): 29 Sep 2020

Highly sensitive optical detection of *Escherichia coli* using Terbium based metal-organic framework

Arushi Gupta[1,2], Mayank Garg[1,2], Suman Singh[1,2], Akash Deep[1, 2*], Amit L Sharma[1, 2*]

[1]CSIR- Central Scientific Instruments Organisation, Sector 30-C, Chandigarh-160030, India

[2]Academy of Scientific and Innovative Research (AcSIR), Ghaziabad-201002, India

[*]Corresponding authors: dr.akashdeep@csio.res.in, amitsharma_csio@csio.res.in

Abstract

Metal-organic frameworks (MOF) are envisaged highly useful for the development of biosensors. Herein, for the first time, we report the optical detection of *Escherichia coli* (*E. coli*) using a water-dispersible Terbium MOF (Tb-BTC, BTC = 1,3,5-benzenetricarboxylic acid). The successful synthesis of Tb-BTC is verified using spectroscopic and morphological techniques like UV-Vis, fluorescence and FTIR spectroscopy, X-Ray diffraction analysis and electron microscopy. Tb-BTC has been bio-interfaced with anti-*E. coli* antibodies and then investigated as a biosensor for *E. coli*. The biosensor displays detection ability in an analyte concentration range of 1.3×10^2 to 1.3×10^8 cfu/mL with a detection limit of 3 cfu/mL, having a response time of 5 min and a total analysis time of about 20-25 min. The results are also found to be reproducible and specific in the presence of some other interfering bacterial species. As demonstrated, the present sensor provides highly sensitive and specific detection of *E. coli* in different samples, including water and fruit juice. To the best of our knowledge, this is the first report to showcase the potential of the MOF based fluorescent biosensor for the detection of *E. coli*.

Keywords: *Tb-BTC MOF, Waterborne pathogen, Escherichia coli, Biosensor, Fluorescence, Real sample.*

1. Introduction

The lack of safe drinking water is a global burden and it affects more than half the population of the developing world. According to the World Health Organization (WHO), approximately 1 billion people lack access to safe drinking water and this problem is estimated to cause more than 2.2 million deaths per year.[1] The disease outbreaks from the polluted water are caused by a variety of microorganisms, such as bacteria, virus, and parasites containing protozoa and helminths. Alarmingly, two-third of these outbreaks are caused by bacteria.[2] Not only the developing nations, but the developed ones are also widely affected by the waterborne pathogens. Some of the bacterial strains are harmless while some even considered beneficial. Several others, being pathogenic in nature, can tremendously impact the socio-economic balance.[3] *Escherichia coli (E. coli)* is one of the microorganisms known to cause harm to the public health. It is a Gram-negative, commensal microorganism usually found in the gut of warm blooded animals, including human .[4] Some strains of *E. coli* are known to cause severe foodborne diseases, urinary tract infection, cholecystitis, bacteremia, and traveler's diarrhea.[5]

Various methods are available for the qualitative and quantitative detection of bacteria. The usually employed methods such as plate counting, Polymerase Chain Reaction based, chemiluminescent *in situ* hybridization, and enzyme-linked immunosorbent assay provide reliable quantification of bacteria in different samples (e.g., water, food, etc.) but they suffer from some disadvantages like long analysis time, use of expensive chemicals, and requirement of trained personnel and sophisticated instruments.[6-9] Biosensors are recognized as more convenient and low-cost options for the detection of bacterial pathogens. For the detection of *E. coli* also, various biosensors have been developed based on the use of different nanomaterials.[10-13] The use of nanomaterials in biosensors is well known to provide enhanced sensitivity and specificity in comparison to other traditional materials.[14-15] A large number

of biosensors developed for *E. coli* are based on electrochemistry.[16-19] The optical biosensors for *E. coli* have been relatively less explored. For instance, molybdenum disulphide (MoS_2) nanosheets based detection has been reported with a limit of detection (LOD) of 94 cfu/mL.[20] The carboxy-functionalized aptameric ink, patterned on nitrocellulose substrate, has been reported with a LOD of 25 cfu/mL.[21] A fluorescent approach of Cu^{2+} triggered oxidation of o-phenlyenediamine has been suggested for the detection of *E. coli* (10^2 to 10^6 cfu/mL) with a LOD of 100 cfu/mL.[22]

In the last decade, metal-organic frameworks (MOFs) have come up on the scene as highly useful luminescent sensors (both chemo- and bio-) for a number of analytes, including cations, anions, emerging pollutants, gases, biomolecules, etc.[23-29] In comparison to other fluorescent nanomaterials (such as quantum dots, metal nanoparticles, etc.), MOFs are characterized with larger surface area, photo stability, enhanced fluorescence yield, tunable and accessible pores, and readily available functional groups.[30] Therefore, MOFs based optical biosensors have been suggested as incredibly useful options.[31-32]

Terbium based MOFs (Tb-MOFs) have been explored in chemo-/bio- sensors because of their favorable material properties.[33-34] Tb-MOFs are easier to synthesize and disperse nicely in solvents, including water. In particular, the aqueous stability of Tb-MOFs is useful in context to their biosensing applications.[35-37] Because of spin- and/or parity-forbidden f-f transitions, emission from Tb ions is generally weak. Nevertheless, Tb-MOFs offer excellent photoluminescence characteristics as the π-conjugated organic linkers (e.g., H_3BTC) allows electron transfer between Tb ions and ligand ions thereby enhancing the emission (antenna effect).[33] Due to the above features of Tb-MOFs, they can deliver enhanced detection sensitivities when used to develop biosensing systems. Tb-MOFs have been reported for the luminescent sensing of dipicolinc acid (DPA), Fe^{3+} ions, etc.[38-39] A water-stable Tb-MOF ($Tb(ppda)(ox)0.5(H_2O)_2$) has been reported for the optical detection of Al^{3+} and Co_3^{2-}

showing detection limits of 5.66 μM and 0.38 μM, respectively.[35] A Tb-MOF, conjugated with aptamer modified gold nanoparticles, has been utilized for the determination of adenosine triphosphate (ATP) over a concentration range of 0.5-10 μM (LOD = 0.32 μM).[40]

Despite their favorable properties as a luminescent sensory material, Tb-MOFs have not been explored for the biosensing of pathogens. In this study, for the first time, we report the use of an antibody conjugated Tb-MOF (Tb-BTC, where BTC = benzene-1,3,5 tricarboxylic acid) biosensor for the fluorescent detection of *E. coli*. Tb-BTC was synthesized by a facile method and subsequently bio-interfaced with anti-*E. coli* antibodies. It has been possible to detect *E. coli* from 1.3×10^2 to 1.3×10^8 cfu with 3 cfu/mL limit of detection (LOD). The test is rapid (total analysis time of 25-30 minutes) and the biosensor shows specific detection capability as well.

2. Experimental

2.1. Chemicals

All the chemicals were high purity products and used without further purification unless specified otherwise. Terbium nitrate ($Tb(NO_3)_3\cdot6H_2O$, 99.99%) and benzene-1,3,5-tricarboxylic acid (trimesic acid, H_3BTC) were purchased from Sigma-Aldrich (India). Anti-*E. coli* antibodies (Polyclonal; *E. coli* 157:H7) were procured from Abcam (India). Nutrient agar was purchased from Himedia, India. The bacterial culture (*Escherichia coli* (MTCC 1302), *Salmonella typhimurium* (MTCC 98), *Staphlyococcus aureus* (MTCC 96)) were procured from the Microbial Type Culture Collection and Gene bank (MTCC) of CSIR-Institute of Microbial Technology (IMTECH), Chandigarh, India. Phosphate buffered saline (PBS) was purchased from Sigma-Aldrich (pH = 7.4). Ultrapure water (18.2 MΩ) was used throughout the experiments.

2.2. Material characterization

The spectroscopic studies were performed using FT-IR (Spectrum Two, Perkin Elmer, USA) and UV-Visible-NIR (Cary 7000, Agilent, USA) spectrophotometers. The structural analysis was investigated using X-ray diffraction (D8 Advance, Bruker, Germany) technique. The fluorescence measurements were carried out using a multimode plate reader (SpectraMax i3X, Molecular Devices, USA). The surface morphology and elemental composition were investigated using a scanning electron microscope (SEM, JEOL JSM-6610LV Japan) and a transmission electron microscope (HRTEM, JEM 2100 Plus, JEOL, Japan).

2.3. Synthesis of Tb-BTC MOF and its bio-conjugation with anti- *E. coli* antibodies

Tb-BTC was synthesized according to a previously published protocol.[41] Briefly, 46 mg of $Tb(NO_3)_3 \cdot 6H_2O$ (0.1 mM) was taken and dissolved in 5 mL of deionized water. Simultaneously, 22 mg of benzene-1,3,5-tricarboxylic acid (H_3BTC, 0.1 mM) was dissolved in 5 mL of ethanol. The prepared $Tb(NO_3)_3 \cdot 6H_2O$ was then added to H_3BTC solution and allowed to react under vigorous stirring at room temperature (RT, 25±2ºC). A white precipitate was formed immediately. The stirring was continued for 60 min and the whole precipitate obtained was collected by centrifugation. The product (Tb-BTC) was washed several times with water and ethanol and then dried at RT.

For bio-conjugation, 1 mg/mL Tb-BTC dispersion (PBS) was left in contact with a mixed solution of 0.05 M [(1-ethyl-3-(3-(dimethylamino)propyl) carbodiimide] (EDC) and 0.01 M [N-hydroxysuccinimide] (NHS). Next, the anti-*E. coli* antibodies (0.1 mg/mL) were added to above mixture and the contents incubated at 4ºC for overnight. The antibody bio-conjugated Tb-BTC (Ab/Tb-BTC) as precipitate after centrifugation and then washed with PBS buffer to remove any unbound antibodies. It was stored under refrigerated conditions.

The summarized approach of MOF preparation, bioconjugation, and fluorescence based analysis of *E. coli* is depicted in the table of content.

2.4. Detection of *E. coli*

The bacterial cultures used in the study were cultured by incubating (shaking) them overnight in Nutrient-Broth medium (37ºC). The optical density at 600 nm ($O.D._{600}$) was measured to estimate the bacterial concentration. The culture was then centrifuged at 6000 rpm for 10 min. The pellet was collected and suspended in PBS buffer. Various concentrations of *E. coli* were prepared by diluting the stock solution in sterile PBS (1.3×10^3 to 1.3×10^9 cfu/mL). The bacterial concentration in the stock concentration was determined with the standard colony counting method. For the biosensing experiments, 100 µL of the prepared *E. coli* solution was added to 120 µL of Ab/Tb-BTC solution and then left to incubate for 10 min at RT. After the incubation, the mixture was centrifuged (5000 rpm) for 10 min to separate the *E. coli* attached Ab/Tb-BTC pellet. The pellet was re-suspended in 1 mL of PBS and the photoluminescence intensity was measured at an excitation wavelength of 292 nm. The response time of the sensor as well as some other quality assessment parameters, were determined against a fixed concentration of *E. coli* (1.3×10^2 cfu/mL).

The specificity of the developed sensor system for *E. coli* (1.3×10^2 cfu/mL) was assessed by analyzing non-specific *S. typhimurium* and *S. aureus* (1.3×10^8 cfu/mL). For the reproducibility study, 5 different batches of photoluminescence Ab/Tb-BTC dispersions were used to analyze 1.3×10^2 cfu/mL *E. coli*. The robustness of the sensor system for the analysis of real samples was evaluated by spiking fruit samples with some known concentrations of *E. coli*.

3. Results and discussion

3.1. Spectrophotometric characterizations

The FT-IR spectrum of Tb-BTC is depicted in Fig. 1(a). The peaks present in the frequency range of 1590-1490 cm^{-1} are due to the asymmetric vibrations of carboxylate groups. The symmetric vibrations of carboxylate group (BTC) can be detected by a peak at 1380 cm^{-1}.[42] A characteristic band around 1700 cm^{-1} could be attributed to the asymmetric stretching vibrations of carboxylate groups. The characteristic peaks of the linker molecule at 1730 -1690 cm^{-1} and 1280 cm^{-1} are not present in the spectrum of Tb-BTC indicating the absence of leftover precursors and thereby indicating a successful formation of Tb-BTC.[43] After the antibodies attachment, FT-IR spectrum displays a small peak at 1635 cm^{-1} depicting amide II vibrations band of protein backbone.[44]

The UV-Vis absorption spectrum of Tb-BTC material is shown in Fig. 1(b). A broad band between 220-300 nm is a typical characteristic signal of Tb-BTC.[45] The peak is attributed to the charge transfer between the oxygen (O^{2-}) and terbium ions (Tb^{3+}) and π–π^* electron transitions of the linker molecule (i.e. BTC).[46]

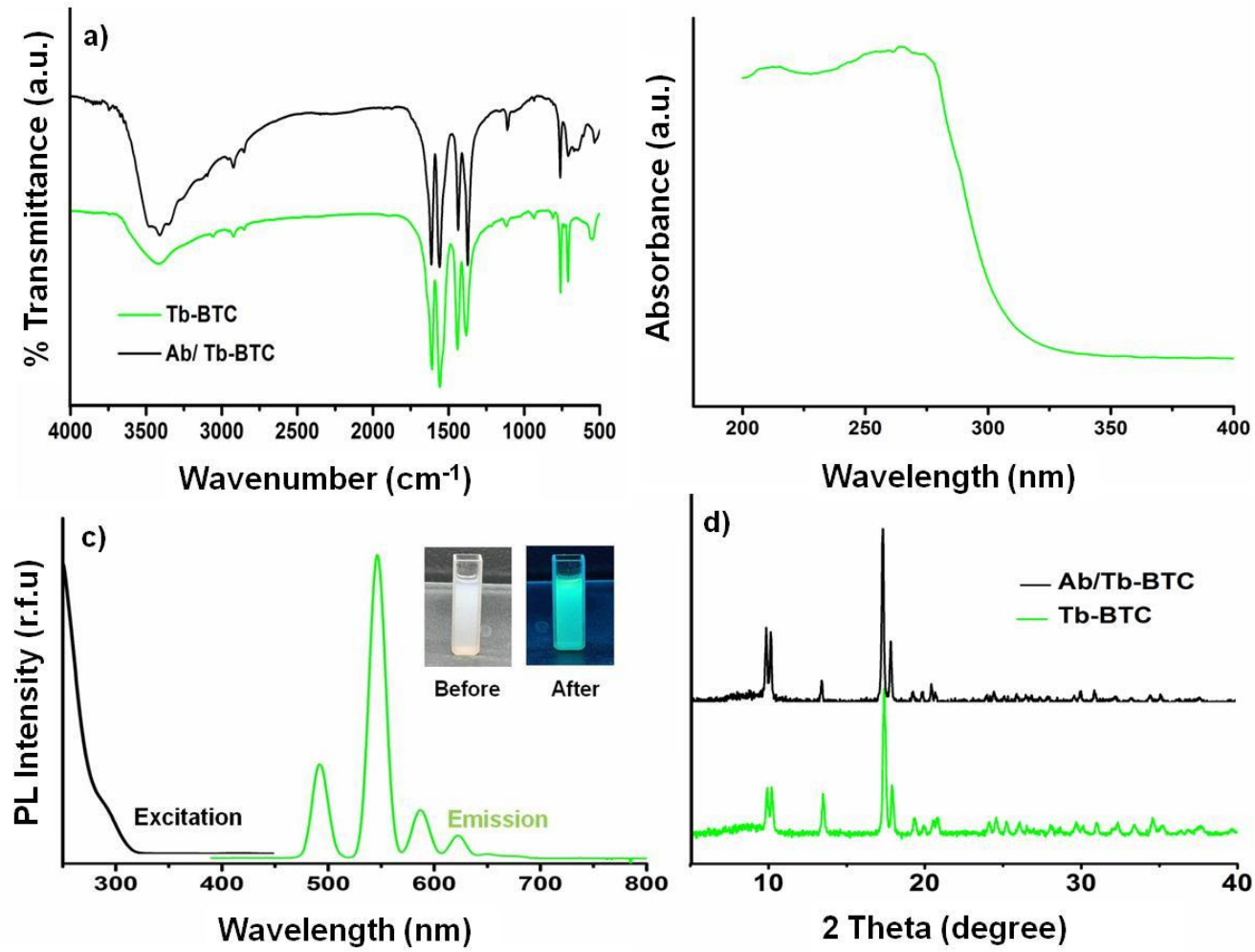

Fig. 1(a): FT-IR spectra of Tb-BTC and Ab/Tb-BTC; (b) UV-vis spectra of Tb-BTC; (c) Excitation and photoluminescence (excitation wavelength = 292 nm) spectra of Tb-BTC (inset showing photograph of Tb-BTC dispersion under UV light irradiation); (d) XRD spectra of Tb-BTC and Ab/Tb-BTC

The photoluminescence (PL) emission studies were also carried out [Fig. 1(c)]. The PL spectrum of Tb-BTC upon excitation with a wavelength energy of 292 nm exhibits a characteristics emission peak of Tb^{3+} ions at 488 nm ascribing to the $^5D_4 \rightarrow {}^7F_6$ transitions. Also, sharp peaks at 546 (most intense band), 581, and 620 nm can be attributed to $^5D_4 \rightarrow {}^7F_5$, $^5D_4 \rightarrow {}^7F_4$, and $^5D_4 \rightarrow {}^7F_3$ transitions, respectively.[41, 47]

3.2. Structural and morphological studies

The structural features of Tb-BTC and Ab/Tb-BTC sample were analyzed by XRD studies [Fig. 1(d)]. Both the samples display sharp diffraction peaks indicative of high degree of crystallinity. The identical XRD patterns confirm the fact that the addition of the antibodies does not alter the structural integrity of Tb-BTC. The 2θ peaks at 8, 9 and 18º are characteristic of Tb-BTC MOF. The crystal structure of Tb-BTC consists of Tb^{3+} ions, trimesate ions, and one coordinated water molecule. Tb^{3+} ions are linked to each other through three O-C-O groups from linker molecule (H_3BTC).[48-49] As all the Tb-BTC related diffraction peaks are also present in Ab/Tb-BTC sample, it is a sufficient evidence about the structural integrity of the bioconjugated Tb-BTC.[50] The morphology of the synthesized MOF was characterized by TEM and element mapping analysis (Fig. 2). The results indicating a rod-shape like morphology of Tb-BTC are in accordance with the previously reported literature.[49] The EDX data [Fig. 2(b)] confirm the presence of Tb ions in the material, thus verifying the successful synthesis of Tb-BTC. The elemental mapping pattern also shows the presence of C, O, and some N [Fig. 2(c-f)].

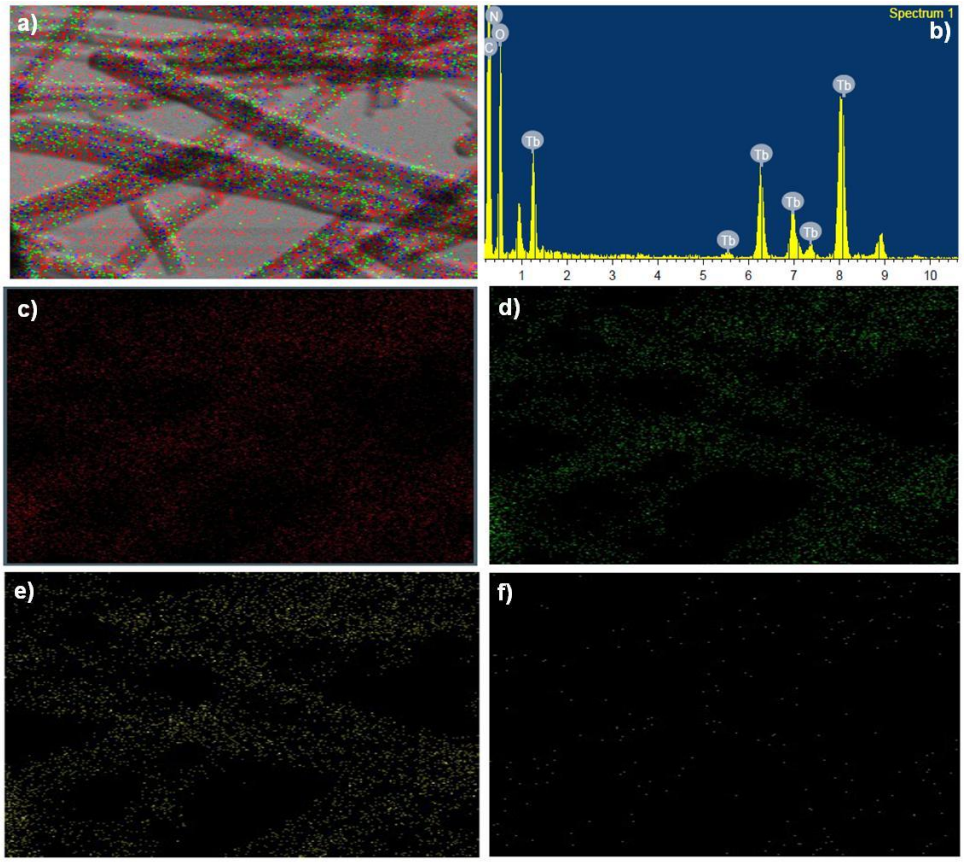

Fig. 2. (a) TEM image of Tb-BTC; (b) EDX spectra of Tb-BTC; (c-f) corresponding elemental mapping patterns [(c) C (d) O (e) Tb (f) N]

3.3. Photoluminescent detection of *E. coli*

The synthesized Tb-BTC was used for the detection of *E. coli*. The photoluminescence (PL) intensity of Tb-BTC decreases after its conjugation with antibodies [Fig. 3(a)]. This decrease in the PL intensity can be attributed to the competitive absorption of excitation energy between Tb-BTC and the attached antibodies. As a result, there is a lesser net energy available to Tb-BTC during the photoexcitation step. Nonetheless, Ab/Tb-BTC dispersion still shows remarkable photoluminescence intensity because of excellent emission characteristics of Tb-BTC MOF [Fig. 3(a)].[51-52]

The synthesized Ab/Tb-BTC molecular probe has been used for the detection of *E. coli*. Fig. 3(b) shows the analysis of different *E. coli* concentrations (1.3×10^2 to 1.3×10^8 cfu/mL, in the final test

aliquot). The PL intensity has been plotted against the *E. coli* concentrations. The emission signal was recorded at 545 nm because of the best PL intensity at this peak. It is observed that as *E. coli* concentrations increase, the PL intensities decrease [Fig. 3(b)]. This can be accounted to the successful antibody-antigen binding. *E. coli* forms a complex with Ab/Tb-BTC, which further attenuates the availability of net excitation energy to Tb-BTC fluorophore. Consequently, a bacterial concentration dependent reduction in the emission intensity is observed. Fig. 4 shows the SEM image of *E. coli*/Ab/Tb-BTC complex. As this sample was dried for SEM analysis, the morphology of the bacteria is disrupted. Nonetheless, the image gives clear indications about the rod-shape like Tb-BTC, tiny globular antibody particles, and ruptured bacteria.

Fig. 3(c) shows a logarithmic linear relationship between the PL intensity and *E. coli* concentrations. The limit of detection (LOD) of the method is estimated by the formula; $3\times S_b/m$, where S_b is the standard deviation of blank measurements and m is the slope of the calibration plot.[53] Using the above expression, the LOD is found to be 3 cfu/mL. It should be noted that the performance of the herein reported Ab/Tb-BTC biosensor for *E. coli* is better or comparable to most of the earlier reported optical biosensors (Table 1).

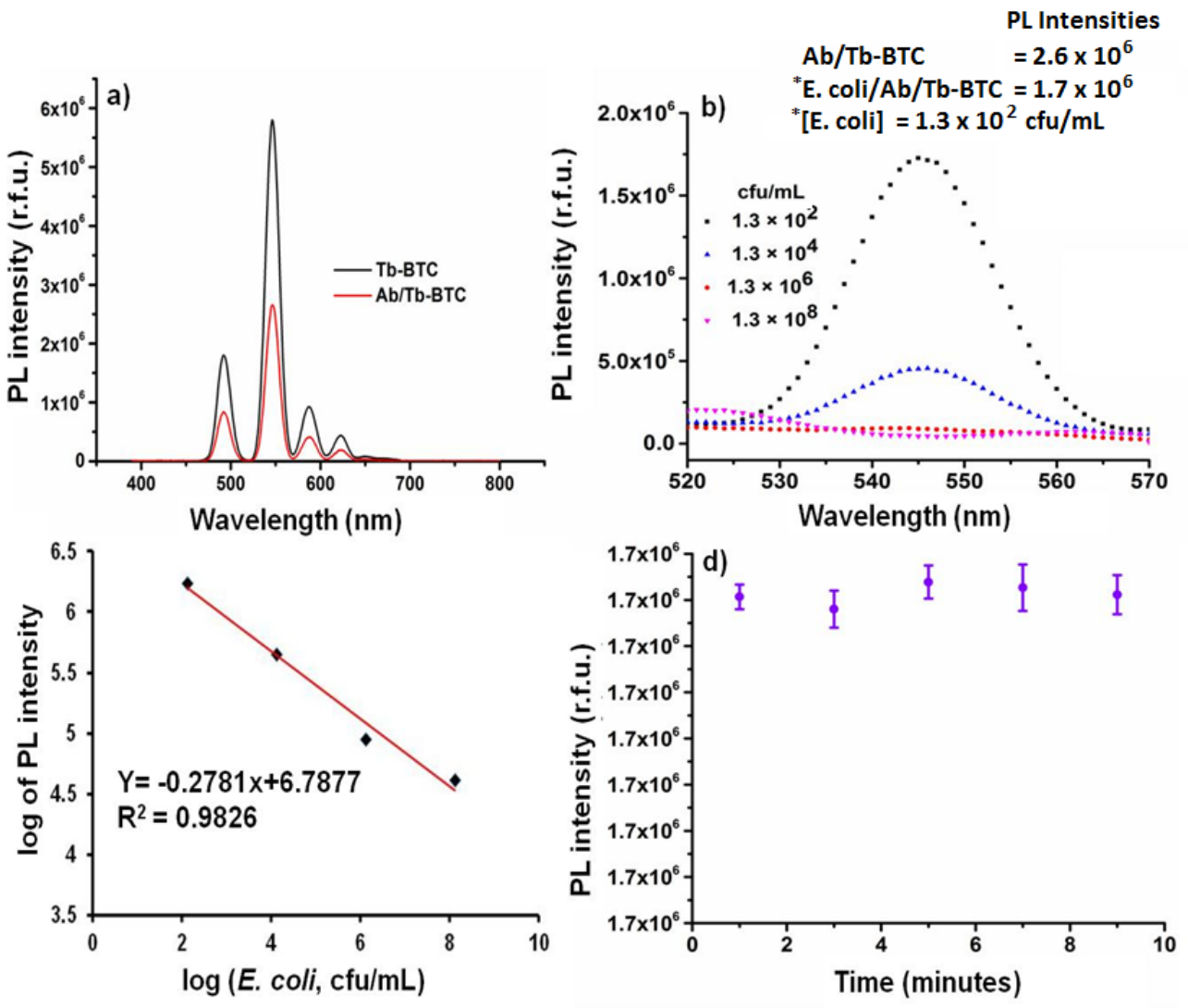

Fig. 3. (a) PL spectra of Tb-BTC and Ab/Tb-BTC; (b) PL spectra of Tb-BTC after the capture and detection of different concentrations of *E. coli* (comparison chart of PL intensities for Ab/Tb-BTC probe and after its complex formation with 1.3×10^2 cfu/mL *E. coli*; (c) Calibration plot; (d) Effect of incubation time between Ab/Tb-BTC and *E. coli* (1.3×10^2 cfu/mL) to generate a stable PL response

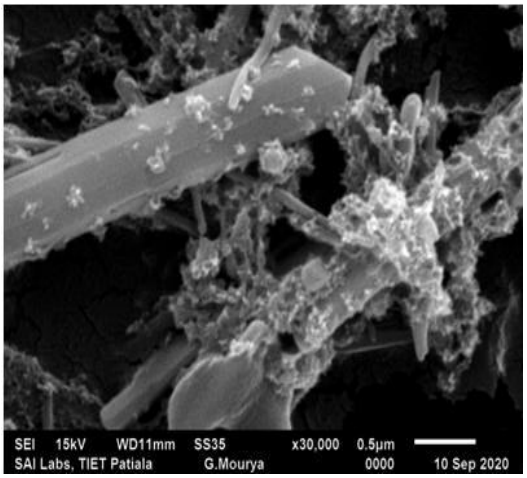

Fig. 4. SEM of *E. coli* bound Ab/Tb-BTC complex. Note that sample was dried for analysis causing rupture of bacteria. Small nanorods are indicative of Tb-BTC structure while small globules highlight the attached antibody particles.

Table 1: Comparative data of the sensing performance of fluorescent biosensors for the detection of *E. coli*.

S.No.	Material	Linear range (cfu/mL)	LOD (cfu/mL)	Ref.
1.	Porous SiO_2	-	10^4	[54]
2.	Gold nanoparticles- reduced graphene oxide	1.0×10^3 to 5.0×10^7	5.0×10^2	[55]
3.	T4 bacteriophage immobilized on microfiber	10^3 to 10^7	10^3	[56]
4.	Oxidised porous SiO_2	-	10^3	[57]
5.	Silicon nanopore array	10^3 to 10^7	-	[58]
6.	Gold-polystyrene particles	10^1 to 10^3	25	[21]
7.	Molybdenum disulfide nanosheets	1000 to 8000	94	[20]
8.	Lateral flow immunoassay strips	10^4 to 10^5	10^4	[59]
9.	**Ab/Tb-MOF**	**1.3×10^2 to 1.3×10^8**	**3**	**Present Work**

3.4. Analysis of merit

The specificity of Ab/Tb-BTC biosensor toward *E. coli* (1.3×10^2 cfu/mL) was studied in the presence of some other interfering organisms such as *S. typhimurium* and *S. aureus* (1.3×10^8 cfu/mL) [Fig. 5(a)]. The PL of Ab/Tb-BTC is quenched only in the presence of *E. coli* while other bacteria do not cause any change in the original PL intensity. The reproducibility of the biosensor response was also studied. For this, five batches of Ab/Tb-BTC biosensor were used for the determination of a fixed bacterial concentration under identical conditions [Fig. 5(b)]. Almost similar results have been obtained in all the cases.

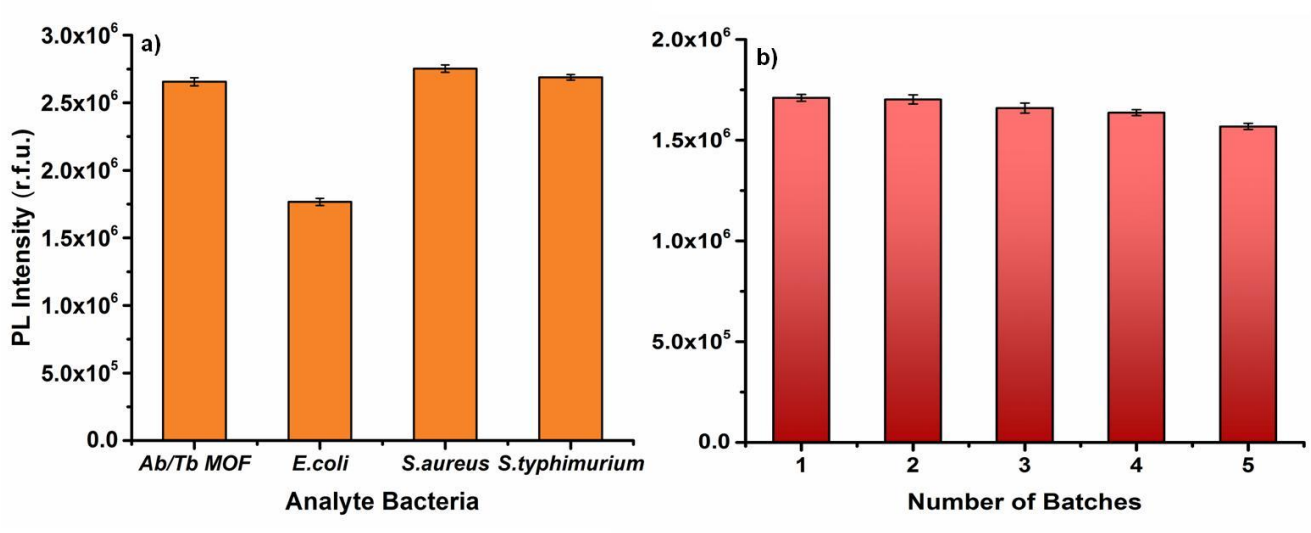

Fig. 5: (a) Specificity of Ab/Tb-BTC toward 1.3×10^2 cfu/mL *E. coli* in presence of other interfering bacteria (*S. typhimurium* and *S. aureus* = 1.3×10^8 cfu/mL) (b) PL signal from different batches of Ab/Tb-BTC when used for the detection of 1.3×10^2 cfu/mL *E. coli*.

The response time of Ab/Tb-BTC biosensor (1 mg/mL) has been studied by incubating it with a fix concentration of *E. coli* (1.3×10^2 cfu/mL) for different time intervals [Fig.3(d)]. A minimum of 5 min is required to achieve a stable degree of photoluminescence quenching. Nonetheless, it should be noted here that the average time for complete analysis (incubation of analyte solution with Ab/Tb-

BTC solution, centrifugation separation, re-suspension, and fluorescence reading) of a sample takes about 20-25 min.

To study the utility of Ab/Tb-BTC biosensor in practical applications, it has been used for the analysis of *E. coli* in a spiked apple juice sample. For preparation, the juice sample was first centrifuged at 10000 rpm for 10 min. The supernatant was collected and then filtered with a syringe filter (0.45 μm).

After the filtration, the prepared sample was spiked with known concentrations of *E. coli* (1.3×10^2 to 1.3×10^8 cfu/mL). The analysis of the spiked juice samples with Ab/Tb-BTC probe was carried out by measuring the PL intensity as a function of the spiked bacterial concentration. The observed PL data was correlated with the standard calibration data. For validation purpose, the bacterial concentration was also determined with the standard colony counting method. As results in Table 2 indicate, the concentration of *E. coli* detected by Ab/Tb-BTC biosensor is in close agreement with the colony counting method. Hence, it can be concluded that Ab/Tb-BTC can be efficiently used for the selective analysis of *E. coli* in different samples.

Table 2: Analysis of *E. coli* in spiked juice samples

Added concentration of *E. coli* (cfu/mL)	Results obtained with colony counting method (cfu/mL)	Results obtained with Ab/Tb-BTC (cfu/mL)
1.3×10^2	1.2×10^2	1.4×10^2
1.3×10^4	1.3×10^4	1.3×10^4
1.3×10^6	1.2×10^6	1.3×10^6
1.3×10^8	1.2×10^8	1.1×10^8

Ab/Tb-BTC has offered convenient and sensitive detection capabilities for *E. coli.* As future scope of study, a solid-state form of Ab/Tb-BTC probe (e.g., paper or strip sensor) can be investigated for the purpose of more user-friendly applications. Its applicability in unprocessed real samples should also be a matter of future research.

4. Conclusion

The present work demonstrates a convenient and an effective antibody conjugated Tb-BTC sensor for rapid and sensitive optical detection of *E. coli*. For the first time, a water dispersible and stable Tb-BTC MOF based photoluminescent immunosensing system is reported for the detection of *E. coli.* Based on PL measurement, the range of detection is 1.3×10^2 to 1.3×10^8 cfu/mL with a low LOD of 3 cfu/mL. Ab/Tb-BTC biosensor has offered a label-free and specific analysis in aqueous and spiked samples. The system is reproducible and equally applicable in real samples. Because of favorable material features, this MOF based optical technique can also be translated in form of disposable strips or portable detection kits for the on-site detection of *E. coli*.

Acknowledgement

The authors are thankful to the Director, CSIR-CSIO, Chandigarh, India for supporting the research work. AG acknowledges the Department of Biotechnology (DBT), Ministry of Science and Technology, Government of India for her research fellowship. MG would like to thank Council of Scientific and Industrial Research (CSIR-HRDG), New Delhi, India for his research fellowship. The research work was funded through a CSIR India grant (MLP-2006).

Conflict of Interest: The authors do not have any conflict of interest to declare.

Author Credit Statement:

Arushi Gupta: Experimental, Data curation, Writing-Original draft preparation; **Mayank Garg:** Experimental, Data curation, Draft preparation; **Suman Singh:** Data interpretation, Writing-Reviewing; **Amit L Sharma:** Data handling, Supervision, Writing-Reviewing; **Akash Deep:** Conceptualization, Project lead, Supervision, Manuscript editing.

References

(1) Kumar, N.; Hu, Y.; Singh, S.; Mizaikoff, B. Emerging biosensor platforms for the assessment of water-borne pathogens. *Analyst* **2018,** *143* (2), 359-373.
(2) Pandey, P. K.; Kass, P. H.; Soupir, M. L.; Biswas, S.; Singh, V. P. Contamination of water resources by pathogenic bacteria. *Amb Express* **2014,** *4* (1), 51.
(3) World Health Organization Mortality and burden of disease from water and sanitation. https://www.who.int/gho/phe/water_sanitation/burden_text/en/(accessed 21 Jan 2020).
(4) Gomes, T. A. T.; Elias, W. P.; Scaletsky, I. C. A.; Guth, B. E. C.; Rodrigues, J. F.; Piazza, R. M. F.; Ferreira, L. C. S.; Martinez, M. B. Diarrheagenic Escherichia coli. *Brazilian Journal of Microbiology* **2016,** *47*, 3-30, DOI: https://doi.org/10.1016/j.bjm.2016.10.015.
(5) Allocati, N.; Masulli, M.; Alexeyev, M. F.; Di Ilio, C. Escherichia coli in Europe: an overview. *International journal of environmental research and public health* **2013,** *10* (12), 6235-6254.
(6) Nurliyana, M. R.; Sahdan, M. Z.; Wibowo, K. M.; Muslihati, A.; Saim, H.; Ahmad, S. A.; Sari, Y.; Mansor, Z. The Detection Method of Escherichia coli in Water Resources: A Review. *Journal of Physics: Conference Series* **2018,** *995*, 012065, DOI: 10.1088/1742-6596/995/1/012065.
(7) Stender, H.; Broomer, A. J.; Oliveira, K.; Perry-O'Keefe, H.; Hyldig-Nielsen, J. J.; Sage, A.; Coull, J. Rapid Detection, Identification, and Enumeration ofEscherichia coli Cells in Municipal Water by Chemiluminescent In Situ Hybridization. *Applied and Environmental Microbiology* **2001,** *67* (1), 142-147, DOI: 10.1128/aem.67.1.142-147.2001.
(8) Molina, F.; López-Acedo, E.; Tabla, R.; Roa, I.; Gómez, A.; Rebollo, J. E. Improved detection of Escherichia coli and coliform bacteria by multiplex PCR. *BMC Biotechnology* **2015,** *15* (1), 48, DOI: 10.1186/s12896-015-0168-2.
(9) Wu, S.-Y.; Hulme, J.; An, S. S. A. Recent trends in the detection of pathogenic Escherichia coli O157 : H7. *BioChip Journal* **2015,** *9* (3), 173-181, DOI: 10.1007/s13206-015-9208-9.
(10) Maas, M. B.; Perold, W.; Dicks, L. Review: Biosensors for the detection of Escherichia coli. *Water SA* **2017,** *43*, 707, DOI: 10.4314/wsa.v43i4.17.
(11) Gupta, A.; Bhardwaj, S. K.; Sharma, A. L.; Deep, A. A graphene electrode functionalized with aminoterephthalic acid for impedimetric immunosensing of Escherichia coli. *Microchimica Acta* **2019,** *186* (12), 800.
(12) Gupta, A.; Bhardwaj, S. K.; Sharma, A. L.; Kim, K.-H.; Deep, A. Development of an advanced electrochemical biosensing platform for E. coli using hybrid metal-organic framework/polyaniline composite. *Environmental research* **2019,** *171*, 395-402.
(13) Thakur, B.; Zhou, G.; Chang, J.; Pu, H.; Jin, B.; Sui, X.; Yuan, X.; Yang, C.-H.; Magruder, M.; Chen, J. Rapid detection of single E. coli bacteria using a graphene-based field-effect transistor device. *Biosensors and Bioelectronics* **2018,** *110*, 16-22.
(14) Mehta, J.; Kumar, R.; Dhaka, S.; Deep, A. Biofunctionalized Nanostructured Materials for Sensing of Pesticides. In *Nanosensors for Environmental Applications*; Springer: 2020; pp 29-86.
(15) Azzouz, A.; Goud, K. Y.; Raza, N.; Ballesteros, E.; Lee, S.-E.; Hong, J.; Deep, A.; Kim, K.-H. Nanomaterial-based electrochemical sensors for the detection of neurochemicals in biological matrices. *TrAC Trends in Analytical Chemistry* **2019,** *110*, 15-34.
(16) Li, Y.; Liu, H.; Huang, H.; Deng, J.; Fang, L.; Luo, J.; Zhang, S.; Huang, J.; Liang, W.; Zheng, J. A sensitive electrochemical strategy via multiple amplification reactions for the detection of E. coli O157: H7. *Biosensors and Bioelectronics* **2020,** *147*, 111752.
(17) Razmi, N.; Hasanzadeh, M.; Willander, M.; Nur, O. Recent Progress on the Electrochemical Biosensing of Escherichia coli O157: H7: Material and Methods Overview. *Biosensors* **2020,** *10* (5), 54.

(18) Zhang, C.; Zhu, F.; Xu, H.; Liu, W.; Yang, L.; Wang, Z.; Ma, J.; Kang, Z.; Liu, Y. Significant improvement of near-UV electroluminescence from ZnO quantum dot LEDs via coupling with carbon nanodot surface plasmons. *Nanoscale* **2017,** *9* (38), 14592-14601.
(19) Güner, A.; Çevik, E.; Şenel, M.; Alpsoy, L. An electrochemical immunosensor for sensitive detection of Escherichia coli O157: H7 by using chitosan, MWCNT, polypyrrole with gold nanoparticles hybrid sensing platform. *Food chemistry* **2017,** *229*, 358-365.
(20) Kaushik, S.; Tiwari, U. K.; Pal, S. S.; Sinha, R. K. Rapid detection of Escherichia coli using fiber optic surface plasmon resonance immunosensor based on biofunctionalized Molybdenum disulfide (MoS2) nanosheets. *Biosensors and Bioelectronics* **2019,** *126*, 501-509.
(21) Díaz-Amaya, S.; Zhao, M.; Lin, L. K.; Ostos, C.; Allebach, J. P.; Chiu, G. T. C.; Deering, A. J.; Stanciu, L. A. Inkjet Printed Nanopatterned Aptamer-Based Sensors for Improved Optical Detection of Foodborne Pathogens. *Small* **2019,** *15* (24), 1805342.
(22) Wang, C.; Gao, X.; Wang, S.; Liu, Y. A smartphone-integrated paper sensing system for fluorescent and colorimetric dual-channel detection of foodborne pathogenic bacteria. *Analytical and Bioanalytical Chemistry* **2020**, 1-10.
(23) Mohanta, G. C.; Bhatt, D.; Deep, A.; Pandey, S. K. Development of Optical Sensor Strips for Point-of-Care Testing for Pesticide. In *Nanosensors for Environmental Applications*; Springer: 2020; pp 225-276.
(24) Mehta, J.; Dhaka, S.; Paul, A. K.; Dayananda, S.; Deep, A. Organophosphate hydrolase conjugated UiO-66-NH2 MOF based highly sensitive optical detection of methyl parathion. *Environmental research* **2019,** *174*, 46-53.
(25) Fang, X.; Zong, B.; Mao, S. Metal–organic framework-based sensors for environmental contaminant sensing. *Nano-micro letters* **2018,** *10* (4), 64.
(26) Strauss, I.; Mundstock, A.; Treger, M.; Lange, K.; Hwang, S.; Chmelik, C.; Rusch, P.; Bigall, N. C.; Pichler, T.; Shiozawa, H. Metal–Organic Framework Co-MOF-74-Based Host–Guest Composites for Resistive Gas Sensing. *ACS applied materials & interfaces* **2019,** *11* (15), 14175-14181.
(27) Anik, Ü.; Timur, S.; Dursun, Z. Metal organic frameworks in electrochemical and optical sensing platforms: a review. *Microchimica Acta* **2019,** *186* (3), 196.
(28) Zhang, X.-J.; Su, F.-Z.; Chen, D.-M.; Peng, Y.; Guo, W.-Y.; Liu, C.-S.; Du, M. A water-stable Eu III-based MOF as a dual-emission luminescent sensor for discriminative detection of nitroaromatic pollutants. *Dalton Transactions* **2019,** *48* (5), 1843-1849.
(29) Samanta, P.; Let, S.; Mandal, W.; Dutta, S.; Ghosh, S. K. Luminescent metal–organic frameworks (LMOFs) as potential probes for the recognition of cationic water pollutants. *Inorganic Chemistry Frontiers* **2020,** *7* (9), 1801-1821.
(30) Bhardwaj, S. K.; Bhardwaj, N.; Kaur, R.; Mehta, J.; Sharma, A. L.; Kim, K.-H.; Deep, A. An overview of different strategies to introduce conductivity in metal–organic frameworks and miscellaneous applications thereof. *Journal of Materials Chemistry A* **2018,** *6* (31), 14992-15009, DOI: 10.1039/C8TA04220A.
(31) Du, L.; Chen, W.; Zhu, P.; Tian, Y.; Chen, Y.; Wu, C. Applications of Functional Metal-Organic Frameworks in Biosensors. *Biotechnology Journal* **2020**, 1900424.
(32) Gonzalez-Gonzalez, E.; Lara-Mayorga, I. M.; Yee-de Leon, F.; Garcia-Rubio, A.; Garciamendez-Mijares, C. E.; Guerra-Alvarez, G. E.; Garcia-Martinez, G.; Aguayo-Hernandez, J. A.; Rodriguez-Sanchez, I. P.; Zhang, Y.-S. Scaling diagnostics in times of COVID-19: Colorimetric Loop-mediated Isothermal Amplification (LAMP) assisted by a 3D-printed incubator for cost-effective and scalable detection of SARS-CoV-2. *medRxiv* **2020**.
(33) Pal, S.; Bharadwaj, P. K. A luminescent terbium MOF containing hydroxyl groups exhibits selective sensing of nitroaromatic compounds and Fe (III) ions. *Crystal Growth & Design* **2016,** *16* (10), 5852-5858.
(34) Qi, Z.; Chen, Y. Charge-transfer-based terbium MOF nanoparticles as fluorescent pH sensor for extreme acidity. *Biosensors and Bioelectronics* **2017,** *87*, 236-241.
(35) Zhan, Z.; Jia, Y.; Li, D.; Zhang, X.; Hu, M. A water-stable terbium-MOF sensor for the selective, sensitive, and recyclable detection of Al 3+ and CO 3 2− ions. *Dalton Transactions* **2019,** *48* (40), 15255-15262.

(36) Cao, L. H.; Shi, F.; Zhang, W. M.; Zang, S. Q.; Mak, T. C. Selective Sensing of Fe3+ and Al3+ Ions and Detection of 2, 4, 6-Trinitrophenol by a Water-Stable Terbium-Based Metal–Organic Framework. *Chemistry–A European Journal* **2015,** *21* (44), 15705-15712.
(37) Wang, Z.; Liu, H.; Wang, S.; Rao, Z.; Yang, Y. A luminescent Terbium-Succinate MOF thin film fabricated by electrodeposition for sensing of Cu2+ in aqueous environment. *Sensors and Actuators B: Chemical* **2015,** *220*, 779-787.
(38) Chen, Z.; Sun, Y.; Zhang, L.; Sun, D.; Liu, F.; Meng, Q.; Wang, R.; Sun, D. A tubular europium–organic framework exhibiting selective sensing of Fe 3+ and Al 3+ over mixed metal ions. *Chemical Communications* **2013,** *49* (98), 11557-11559.
(39) Pellegrino, P. M.; Fell, N. F.; Rosen, D. L.; Gillespie, J. B. Bacterial endospore detection using terbium dipicolinate photoluminescence in the presence of chemical and biological materials. *Analytical Chemistry* **1998,** *70* (9), 1755-1760.
(40) Sun, C.; Zhao, S.; Qu, F.; Han, W.; You, J. Determination of adenosine triphosphate based on the use of fluorescent terbium (III) organic frameworks and aptamer modified gold nanoparticles. *Microchimica Acta* **2020,** *187* (1), 34.
(41) Yang, W.; Feng, J.; Zhang, H. Facile and rapid fabrication of nanostructured lanthanide coordination polymers as selective luminescent probes in aqueous solution. *Journal of Materials Chemistry* **2012,** *22* (14), 6819-6823.
(42) Goel, N.; Kumar, N. A dual-functional luminescent Tb (III) metal–organic framework for the selective sensing of acetone and TNP in water. *RSC advances* **2018,** *8* (20), 10746-10755.
(43) Huangfu, M.; Tian, X.; Zhao, S.; Wu, P.; Chu, H.; Zheng, X.; Tang, J.; Wang, J. Post-Synthetic Modification of Tb-based Metal–Organic Framework for Highly Selective and Sensitive Detection of Metal Ions in Aqueous Solution. *New Journal of Chemistry* **2019**.
(44) Huy, T. Q.; Hanh, N. T. H.; Thuy, N. T.; Van Chung, P.; Nga, P. T.; Tuan, M. A. A novel biosensor based on serum antibody immobilization for rapid detection of viral antigens. *Talanta* **2011,** *86*, 271-277.
(45) Zhang, J.; Peh, S. B.; Wang, J.; Du, Y.; Xi, S.; Dong, J.; Karmakar, A.; Ying, Y.; Wang, Y.; Zhao, D. Hybrid MOF-808-Tb nanospheres for highly sensitive and selective detection of acetone vapor and Fe 3+ in aqueous solution. *Chemical Communications* **2019,** *55* (32), 4727-4730.
(46) Zhang, M.; Han, J.; Wu, H.; Wei, Q.; Xie, G.; Chen, S.; Gao, S. Tb-MOF: a naked-eye and regenerable fluorescent probe for selective and quantitative detection of Fe 3+ and Al 3+ ions. *RSC Advances* **2016,** *6* (97), 94622-94628.
(47) Bhardwaj, N.; Bhardwaj, S.; Mehta, J.; Kim, K.-H.; Deep, A. Highly sensitive detection of dipicolinic acid with a water-dispersible terbium-metal organic framework. *Biosensors and Bioelectronics* **2016,** *86*, 799-804.
(48) Lee, T.; Lee, H. L.; Tsai, M. H.; Cheng, S.-L.; Lee, S.-W.; Hu, J.-C.; Chen, L.-T. A biomimetic tongue by photoluminescent metal–organic frameworks. *Biosensors and Bioelectronics* **2013,** *43*, 56-62.
(49) Fonseca, R. R.; Gaspar, R. D.; Raimundo Jr, I. M.; Luz, P. P. Photoluminescent Tb3+-based metal-organic framework as a sensor for detection of methanol in ethanol fuel. *Journal of Rare Earths* **2019,** *37* (3), 225-231.
(50) Wan, Y.; Sun, W.; Liu, J.; Liu, Z. A 3D porous luminescent terbium metal-organic framework for selective sensing of F− in aqueous solution. *Inorganic Chemistry Communications* **2017,** *80*, 53-57.
(51) Bhardwaj, N.; Bhardwaj, S. K.; Bhatt, D.; Tuteja, S. K.; Kim, K.-H.; Deep, A. Highly sensitive optical biosensing of Staphylococcus aureus with an antibody/metal–organic framework bioconjugate. *Analytical methods* **2019,** *11* (7), 917-923.
(52) Shahrokhian, S.; Ranjbar, S. Aptamer immobilization on amino-functionalized metal–organic frameworks: an ultrasensitive platform for the electrochemical diagnostic of Escherichia coli O157: H7. *Analyst* **2018,** *143* (13), 3191-3201.
(53) Shrivastava, A.; Gupta, V. B. Methods for the determination of limit of detection and limit of quantitation of the analytical methods. *Chronicles of young scientists* **2011,** *2* (1), 21.

(54) Massad-Ivanir, N.; Shtenberg, G.; Segal, E. Optical detection of E. coli bacteria by mesoporous silicon biosensors. *JoVE (Journal of Visualized Experiments)* **2013,** (81), e50805.
(55) Zhou, C.; Zou, H.; Li, M.; Sun, C.; Ren, D.; Li, Y. Fiber optic surface plasmon resonance sensor for detection of E. coli O157: H7 based on antimicrobial peptides and AgNPs-rGO. *Biosensors and Bioelectronics* **2018,** *117*, 347-353.
(56) Li, Y.; Sun, Q.; Luo, Y.; Li, Y.; Gong, A.; Zhang, H.; Liu, D. In *High sensitive and selective Escherichia coli detection using immobilized optical fiber microprobe*, 2017 25th Optical Fiber Sensors Conference (OFS), IEEE: 2017; pp 1-4.
(57) Tenenbaum, E.; Segal, E. Optical biosensors for bacteria detection by a peptidomimetic antimicrobial compound. *Analyst* **2015,** *140* (22), 7726-7733.
(58) Tang, Y.; Li, Z.; Luo, Q.; Liu, J.; Wu, J. Bacteria detection based on its blockage effect on silicon nanopore array. *Biosensors and Bioelectronics* **2016,** *79*, 715-720.
(59) Jung, Y.; Heo, Y.; Lee, J. J.; Deering, A.; Bae, E. Smartphone-based lateral flow imaging system for detection of food-borne bacteria E. coli O157: H7. *Journal of Microbiological Methods* **2020,** *168*, 105800.

Table of Contents